

Detectability of Molecular Signatures on TRAPPIST-1e through Transmission Spectroscopy Simulated for Future Space- Based Observatories

DARIA PIDHORODETSKA,^{1,2,3} THOMAS J. FAUCHEZ,^{1,4,3} GERONIMO L. VILLANUEVA,^{1,3}
SHAWN D. DOMAGAL-GOLDMAN,^{1,3} AND RAVI K. KOPPARAPU^{1,3}

¹*NASA Goddard Space Flight Center*

8800 Greenbelt Road

Greenbelt, MD 20771, USA

²*University of Maryland Baltimore County/CRESST II*

1000 Hilltop Cir.

Baltimore, MD 21250, USA

³*GSFC Sellers Exoplanet Environments Collaboration*

⁴*Goddard Earth Sciences Technology and Research (GESTAR), Universities Space Research Association, Columbia, MD, USA*

(Accepted to ApJ Letters July 2020)

ABSTRACT

Discoveries of terrestrial, Earth-sized exoplanets that lie within the habitable zone (HZ) of their host stars continue to occur at increasing rates. Transit spectroscopy can potentially enable the detection of molecular signatures from such worlds, providing an indication of the presence of an atmosphere and its chemical composition, including gases potentially indicative of a biosphere. Such planets around nearby M-dwarf stars - such as TRAPPIST-1 - provide relatively good signal, high signal/noise, and frequent transits for follow-up spectroscopy. However, even with these advantages, transit spectroscopy of terrestrial planets in the HZ of nearby M-stars will still be a challenge. Herein, we examine the potential for future space observatories to conduct such observations, using a Global Climate Model (GCM), a photochemical model, and

a radiative transfer suite to simulate modern-Earth-like atmospheric boundary conditions on TRAPPIST-1e. The detectability of biosignatures on such an atmosphere via transmission spectroscopy is modeled for various instruments of *JWST*, *LUVVOIR*, *HabEx*, and *Origins*. We show that only CO₂ at 4.3 μm would be detectable at the $> 5 \sigma$ level in transmission spectroscopy, when clouds are included in our simulations. This is because the impacts of clouds on scale height strongly limits the detectability of molecules in the atmosphere. Synergies between space- and ground-based spectroscopy may be essential in order to overcome these difficulties.

Keywords: exoplanets: atmospheres, terrestrial planets, transit spectroscopy, stars:
low-mass, techniques: atmospheric modeling

1. INTRODUCTION

The search for small, Earth-like rocky exoplanets has made significant progress since the launch of *Kepler* in 2009. To date, there are over 4,000 confirmed exoplanets orbiting a multitude of stars, with additional candidates and planets identified frequently. As we continue to detect terrestrial exoplanets that resemble Earth in size, some of the most exciting discoveries point towards planets that fall within the habitable zone (HZ), the region around a star where surface water oceans may be stable under the correct conditions (Kasting et al. 1993; Kopparapu et al. 2013). Such detections have thus far been biased to low mass stars (late-K and M-dwarf stars), as their small size and compact HZs give way to planets with short orbital periods that provide a high frequency of transits. It has been estimated that 16% of early M-dwarf stars and 64% of mid M-dwarf stars contain terrestrial-sized planets orbiting within the habitable zone (Dressing & Charbonneau 2015; Vanderburg et al. 2020). While both radial velocity and transit techniques have revealed the first rocky exoplanets orbiting within the HZ of their low-mass host stars (Anglada-Escudé et al. 2016; Gillon et al. 2016, 2017), the majority of planets discovered through the transit method, specifically, orbit extremely close to their host star (Kaltenegger et al. 2012). This bias has influenced the discovery of many rocky planets orbiting M-type stars. Fortunately, the same observational bias that has led to the detection of these

worlds will also make them more amenable to follow-up characterization, including the identification of atmospheric species via transit spectroscopy (Pallé 2018).

For some exoplanets, transit spectroscopy and/or secondary eclipse measurements (primarily done from space with the *Hubble Space Telescope* (*HST*) and the *Spitzer Space Telescope*) have provided empirical details on their atmospheric compositions (e.g. Seager & Deming 2010; Sing et al. 2016). These investigations have primarily targeted "hot Jupiters" - gas-giant planets with orbital periods of only a few days (e.g. Sing et al. 2011, 2013, 2015; Pont et al. 2013; Gibson et al. 2013; Nikolov et al. 2015; Evans et al. 2018). Several sub-Neptune and super-Earth type planets have also been targeted for atmospheric characterization (e.g. Kreidberg et al. 2014; Knutson et al. 2014; Bourrier et al. 2018; Wakeford et al. 2018; Benneke et al. 2019a,b). However, as discoveries of rocky exoplanets both within and outside of the HZ continue to increase, the first attempts to put constraints on their atmospheric properties with transit spectroscopy measurements have begun (e.g. de Wit et al. 2016, 2018; Southworth et al. 2017; Delrez et al. 2018; Ducrot et al. 2018, 2020; Diamond-Lowe et al. 2018, 2020; Burdanov et al. 2019).

Within this assortment of planets, one of the most exciting and nearby exoplanetary systems that is a target for future observations is the TRAPPIST-1 system (Gillon et al. 2016, 2017). Bearing seven Earth-sized exoplanets (Gillon et al. 2017) orbiting an ultra-cool late-type M-dwarf star (M8V; Liebert & Gizis (2006)) located 12.4 parsec from Earth (Lindgren et al. 2018), the TRAPPIST-1 planets are similar in size and irradiation to the rocky planets within our Solar System (Gillon et al. 2017). Their ultra-cool, low-mass parent star signifies that the evolution of their existence and the pathways they undertook to form are potentially much different than what our Solar System planets experienced (Turbet et al. 2018). This leaves us with the ideal laboratory to study how the atmospheric evolution of a planet orbiting an M-dwarf star can impact its habitability (Wolf 2017; Lincowski et al. 2018; Turbet et al. 2018). Among the seven planets, 3-D climate simulations have shown that TRAPPIST-1e could be the most habitable planet of the system, able to maintain liquid

water on its surface across a large range of atmospheric compositions (Wolf 2017; Turbet et al. 2018; Fauchez et al. 2019a; Fauchez et al. 2019b). This makes it an ideal target to search for the presence of biosignatures, molecular features that may indicate evidence of life.

For the TRAPPIST-1 system, data obtained by *HST* provide initial constraints on the extent and composition of the planet’s atmospheres, suggesting that the four innermost planets do not have a cloud/haze-free H₂-dominated atmosphere (de Wit et al. 2016, 2018). However, follow up work by Moran et al. (2018) have shown that *HST* data can also be fit to a cloudy/hazy H₂-dominated atmosphere. Complementary to *HST*, NASA’s *Spitzer Space Telescope* - which played a major role in the discovery and orbital determination of TRAPPIST-1d, e, f, and g (Gillon et al. 2017) - has also allowed us to put additional constraints on the atmospheric composition of TRAPPIST-1b. Transit observations with *Spitzer* (Delrez et al. 2018) have found a $+208 \pm 110$ ppm difference between the 3.6 and 4.2 μm bands, suggesting CO₂ absorption. *Spitzer* also showed that transit depth measurements do not show any hint of significant stellar contamination in the 4.5 μm spectral range. Morris et al. (2018) reached the same conclusion using a ”self-contamination” approach based on the *Spitzer* data set. *Spitzer*’s ”Red Worlds” Program encompassed over 1000 hours of observations of the TRAPPIST-1 system, whose global results have been presented (Ducrot et al. 2020). *HST* and *Spitzer* measurements have also been combined with transit light curves obtained from space with *K2* (Luger et al. 2017) and from the ground with SPECULOOS-South Observatory (*SSO*; Burdanov et al. 2018; Gillon 2018) and Liverpool Telescope (*LT*; Steele et al. 2004) where Ducrot et al. (2018) produced featureless transmission spectra for the planets in the 0.8 – 4.5 μm wavelength range, showing an absence of significant temporal variations of the transit depths in the visible. Additional ground-based observations with the *United Kingdom Infra – Red Telescope* (*UKIRT*), *Anglo – Australian Telescope* (*AAT*), and *Very Large Telescope* (*VLT*) also show no substantial temporal variations of transit depths for TRAPPIST-1 b, c, e, and g (Burdanov et al. 2019). While the *K2* optical data set detected a 3.3 day periodic 1 % photometric modulation, it is not present in the *Spitzer* observations (Delrez et al. 2018). Further constraints on the molecular

weight and presence/absence of atmospheres on the TRAPPIST-1 planets will require additional observations with future facilities.

The next generation of observatories will allow for far more in-depth explorations of atmospheric properties of the TRAPPIST-1 planets. In particular, data from the *James Webb Space Telescope* (*JWST*) could provide strong constraints on atmospheric temperatures and on the abundances of molecules with large absorption bands (Gillon et al. 2016). *JWST* houses two science instruments capable of using transit spectroscopy to detect light from planets and their host stars: The Near-Infrared Spectrograph (NIRSpec; Bagnasco et al. 2007; Ferruit et al. 2014) and Mid-Infrared Instrument (MIRI; Bouchet et al. 2015) low resolution spectrometer (LRS; Kendrew et al. 2015). NIRSpec, which will cover the infrared wavelength range from 0.6-5.3 μm , intends to analyze the spectrum of over 100 objects observed simultaneously. MIRI has both a camera and a spectrograph that perform between the range of 5-28 μm , with transit observations ending at 12 μm . Only the low resolution spectroscopy (LRS) mode allows for time series observations with MIRI.

Prior studies have evaluated the potential of *JWST* to characterize the TRAPPIST-1 planets (Lincowski et al. 2018; Lustig-Yaeger et al. 2019). Morley et al. (2017) determined that less than 20 transits are needed to rule out a flat line with a confidence level of 5σ if the atmosphere is CO_2 -dominated on six of the seven TRAPPIST-1 planets. However, *JWST's* ability to characterize *individual* molecular features using transit spectroscopy will be much more limited. This is partially due to the effects of clouds (Suisa et al. 2019a; Komacek et al. 2019; Fauchez et al. 2019a). CO_2 could be the only gas in a HZ terrestrial planet's atmosphere that can be detected (Lustig-Yaeger et al. 2019; Fauchez et al. 2019a). For other atmospheric states, other gases may also be detectable. For example, at higher abundances, CH_4 (Lustig-Yaeger et al. 2019) and $\text{O}_2\text{-O}_2$ collision-induced absorption (CIA; Misra et al. 2014; Lustig-Yaeger et al. 2019; Fauchez et al. 2019c) might also be detectable by *JWST*.

Biosignature detection with *JWST* has also been modeled explicitly for methanogen-dominated biospheres that produce high CH_4 concentrations. The combination of high CO_2 and high CH_4 is a potential biosignature for an Archean-like world (Arney et al. 2016; Krissansen-Totton et al. 2016), because the CH_4 fluxes required to sustain CH_4 in the presence of high CO_2 concentrations are orders of magnitude greater than fluxes that are consistent with geological activity. For planets with biospheres more similar to the one on modern-day Earth, *JWST* may not be able to detect any biosignatures, if clouds are present in the planet’s atmosphere (Komacek et al. 2019; Fauchez et al. 2019a).

In 2016, the Astrophysics Division in NASA’s Science Mission Directorate commissioned the study of four large concepts in preparation for the 2020 Astrophysics Decadal Survey. In this work, we simulate and compare with respect to *JWST* the transit spectroscopy performances of three of those concept missions: the *Large UV/Optical/Infrared Surveyor* (*LUVOIR*; TheLUVOIRTeam 2019), the *Habitable Exoplanet Observatory* (*HabEx*; Gaudi et al. 2018), and *Origins* (Meixner et al. (2019); formerly the Far-Infrared Surveyor). Any of the concepts that are prioritized in the Decadal Survey will have a proposed launch date in the 2030s.

LUVOIR:—*LUVOIR* is a concept for a large, multi-wavelength ($0.1\text{--}2.5\ \mu\text{m}$) serviceable observatory following the heritage of *HST*. *LUVOIR*’s current proposed architecture is a scalable observatory whose eventual size would fall within a range defined by two point design concepts: *LUVOIR*-A consists of an on-axis, large (15 m) segmented aperture telescope while *LUVOIR*-B consists of an off-axis, large (8 m) segmented aperture. The notional instrument for transit observations in the near-UV and near-IR is the High Definition Imager (HDI, $0.2\text{--}2.5\ \mu\text{m}$; TheLUVOIRTeam (2019)).

HabEx:—While *HabEx* proposes a multitude of architectures, this work simulated the baseline architecture, which includes a 4-m monolithic, off-axis telescope concept with a wavelength range of $0.1\text{--}1.8\ \mu\text{m}$. *HabEx* is equipped with a suite of four proposed instruments that demonstrate various

science capabilities, but the most relevant instrument for transit spectroscopy work is the HabEx Workhorse Camera (HWC, 0.2-1.8 μm ; [Gaudi et al. \(2018\)](#)).

Origins:—The current design concept for *Origins* is a 5.9 m on-axis telescope with a *Spitzer*-like structure that allows for minimal deployment while having a collecting area nearly equivalent in size to that of *JWST* ([Battersby et al. 2018](#)). Observations with *Origins* intend to cover a broad wavelength range (3-600 μm) with instruments that have an improved sensitivity compared to *JWST*, mainly due to the greatly reduced telescope temperature (<5 K). *Origins* proposes multiple science instruments, but the most appropriate for conducting transmission spectroscopy measurements is the Mid-Infrared Spectrometer Camera-Transit Spectrometer (MISC-T, 2.8-20 μm ; [Meixner et al. \(2019\)](#)).

The objective of this work is to cross-compare the capability of each of these future space-based missions to characterize a modern Earth-like TRAPPIST-1e (or an equivalent potentially habitable transiting M-dwarf exoplanet) via transmission spectroscopy. The paper is structured as follows: Section 2 discusses the method and the tools used in this study to simulate both the climate and the transmission spectra of TRAPPIST-1e. Section 3 presents the results of our simulations, identifying each gaseous signature in the spectra and their detectability with future observatories. Discussions of our results are provided in Section 4. Finally, conclusions and perspectives are presented in Section 5.

2. MODELS AND METHODS

In the following subsections, we describe our methods for assessing the signal-to-noise ratio (S/N) of various molecular signatures for TRAPPIST-1e with numerous instruments and observational modes available to *JWST*, *LUVOIR*, *HabEx*, and *Origins*. Although there is a significant parameter space to be explored regarding the potential atmospheric scenarios for temperate terrestrial planets, this work examines the detectability of a modern Earth-like atmosphere, both with and without the presence of aerosols. Each atmospheric configuration is created with the LMD-Generic Global

Climate Model (GCM; [Wordsworth et al. 2011](#)), and is then analyzed using the Planetary Spectrum Generator (PSG; <https://psg.gsfc.nasa.gov>), an online radiative-transfer suite that computes synthetic transit spectra for a wide range of objects such as planets, moons, comets, and asteroids ([Villanueva et al. 2018](#)). We aim to determine how feasible the detection and characterization of a modern Earth-like atmosphere would be for *JWST*, and we assess how the feasibility of its detection may be improved with observations from future observatories. We consider an atmosphere to be detected when sufficient S/N is achieved on the strongest molecular feature in the spectrum at a 5σ confidence level.

2.1. *Climate simulations with the LMD-Generic Global Climate Model (GCM)*

This work employs the 3-D Global Climate Model (GCM) developed and maintained at the Laboratoire de Mtorologie Dynamique (LMD), specifically their generic GCM, LMD-G. We use LMD-G to simulate an atmosphere with the same composition as modern Earth. We use modern Earth, because it is the only example of a globally habitable planet, and is therefore also the most well-studied example of one. As such, modern Earth is the most widespread benchmark for habitable planets in the literature (e.g., [Barstow & Irwin 2016](#); [Morley et al. 2017](#); [Lincowski et al. 2018](#)).

Details on LMD-G can be found in [Turbet et al. \(2018\)](#); [Fauchez et al. \(2019a\)](#). In this work, we have performed climate simulations of TRAPPIST-1e using the stellar and planetary parameters from ([Gillon et al. 2017](#); [Grimm et al. 2018](#)). Herein, TRAPPIST-1e is assumed to be fully covered by a 100 m deep ocean (aqua-planet) with a thermal inertia of $12000 \text{ J} \cdot \text{m}^{-2} \cdot \text{K}^{-1} \cdot \text{s}^{-2}$ without ocean heat transport (OHT). TRAPPIST-1e is also assumed to be in synchronous rotation. The horizontal resolution of the model is 64×48 coordinates in longitude \times latitude (e.g., $5.6^\circ \times 3.8^\circ$). In the vertical direction, the atmosphere is discretized in 26 distinct layers using the hybrid σ coordinates (with the top of the model at 10^{-5} bar) while the ocean is discretized in 18 layers. The stellar TRAPPIST-1 emission spectrum was computed using the synthetic BT-Settl spectrum ([Rajpurohit et al. 2013](#)) assuming a temperature of 2500 K, a surface gravity of $10^3 \text{ m} \cdot \text{s}^{-2}$, and a metallicity of 0 dex. These

stellar parameters have been selected to be consistent with the [Turbet et al. \(2017\)](#) and [Fauchez et al. \(2019a\)](#) simulations of the TRAPPIST-1 system with the LMD-G GCM.

2.2. Photochemistry simulations with the Atmos Model

The LMD-G GCM, like most GCMs used in exoplanet research, does not include photochemistry prognostically. Therefore, in order to simulate an atmospheric composition more complex than the one provided by the GCM, we utilize a 1-D photochemistry code, Atmos, to produce vertical chemical profiles. Atmos is a 1-D radiative-convective climate model, coupled with a 1-D photochemistry model, capable of simulating a variety of atmospheric redox states ([Arney et al. 2016, 2017](#); [Lincowski et al. 2018](#); [Meadows et al. 2018](#)). The boundary conditions in Atmos for modern Earth-like planets are described in [Fauchez et al. \(2019a\)](#) Table 2, adapted from [Lincowski et al. \(2018\)](#) in Table 8, except for the H₂O and cloud profiles, which have been directly provided from the LMD-G GCM outputs. Photochemistry calculations have been performed at the terminator only (longitude $\pm 90^\circ$) where the star light is transmitted through the atmosphere. Atmos uses the temperature/pressure profiles and mixing ratios from the LMD-G outputs for each latitude coordinate around the terminator as used in [Fauchez et al. \(2019a\)](#). Figure 1 shows the mixing ratios computed for various gases when the photochemical model has converged. Gaseous profiles at the terminator are then used to compute transmission spectra with PSG.

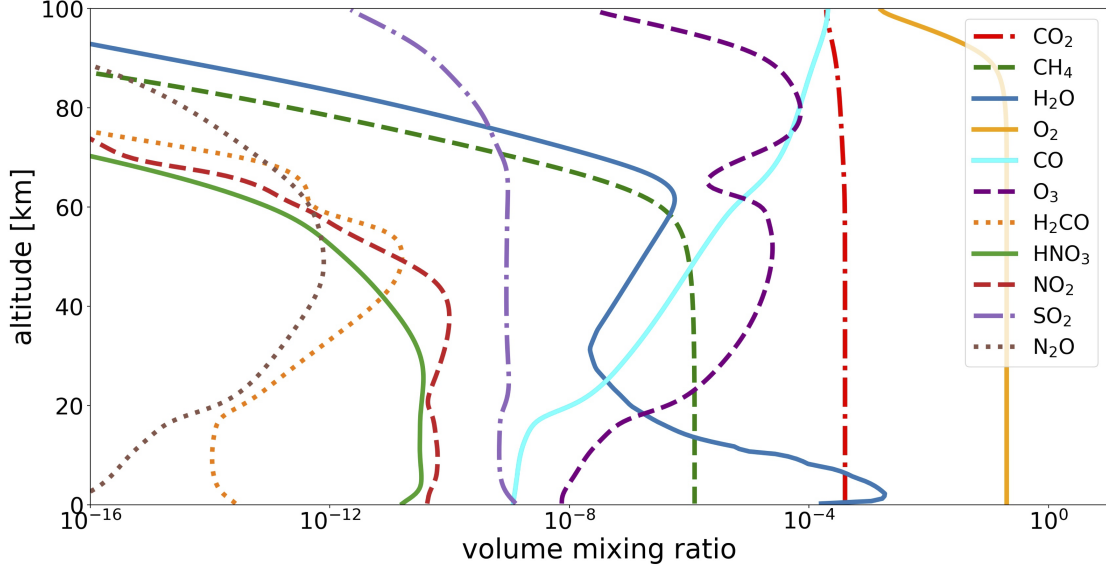


Figure 1. Terminator-averaged gaseous atmospheric profiles for modern Earth-like boundary conditions on TRAPPIST-1e with abiotic fluxes (except for O_2 with a fixed mixing ratio of 0.21) produced by Atmos. The CO_2 vertical mixing ratio is constant, while most other gases are depleted due to photodissociation at higher altitudes. N_2 is excluded here as it has a fixed mixing ratio of 0.78 and is not involved in any photochemical reactions.

2.3. The Planetary Spectrum Generator (PSG)

To create simulated spectra from our model inputs, we use PSG, a publicly available tool found online at <https://psg.gsfc.nasa.gov/> (Villanueva et al. 2018). PSG is a spectroscopic suite that integrates the latest radiative transfer methods and spectroscopic parameterizations while including a realistic treatment of multiple scattering in layer-by-layer pseudo-spherical geometry (Villanueva et al. 2018). PSG permits the ingestion of billions of spectral lines of over 1,000 molecular species from several spectroscopic repositories (e.g., HITRAN, JPL, CDMS, GSFC-Fluor). For this investigation, the molecular spectroscopy is based on the latest HITRAN database (Gordon et al. 2017), which is complemented by UV/optical data from the MPI database (Keller-Rudek et al. 2013). For moderate spectral resolutions ($\lambda/\Delta\lambda < 5000$) as those presented here, PSG applies the correlated-k technique for the radiative transfer portion, while multiple scattering from aerosols is performed by PSG using the discrete ordinates method, in which the radiation field is approximated by a discrete

number of streams distributed in an angle with respect to the plane-parallel normal.

PSG allows the user to explore many different instrument modes across a multitude of observatories. Using pre-loaded templates, PSG accounts for system throughput and presents the user with a table that describes these values, all of which are found in the detector parameters. In all synthetic spectra shown within this work, the resolving power (R) selected for each instrument is varied to accommodate the most efficient detection of the strongest molecular feature found within the spectrum of a given atmosphere. Each simulation is then plotted over a higher resolution ($R = 100$) model. We compute the visibility of TRAPPIST-1e within a 5-year timespan, giving us 85 observable transits. This value is fixed for each S/N calculation.

To estimate the S/N of a specific spectral line, we subtract the relative transit depth value of the line peak ($\delta\Delta_l$) from the transit depth value of the nearest continuum ($\delta\Delta_c$) - the latter could significantly vary in the VIS due to the Rayleigh slope - giving us our signal (S). We then divide S by the value of the noise of the relative transit depth ($N^{\delta\Delta_l}$) of the line peak (l). We mathematically express this as:

$$S/N = (\delta\Delta_l - \delta\Delta_c) / N^{\delta\Delta_l} \quad (1)$$

In order to properly capture the diversity of atmospheric conditions at the terminator as computed by the GCM, the transit spectra presented in this work were computed by running PSG at each lat-lon bin at the terminator of the planet. Information about temperature, pressure and abundance profiles at each lat-lon gridpoint from the GCM were ported into the input parameters for the spectroscopic simulations performed with PSG. These individual transit spectra were then averaged to compute the total planetary transit spectra. Considering that the spacing of the latitudinal points is constant in the GCM, the integration weights for each spectrum were assumed to be equal, and a simple average of the transit spectra was performed.

3. RESULTS

3.1. *Identification of Spectral Lines for a Modern Earth-like Atmosphere on TRAPPIST-1e*

Figure 2 represents the transmission spectrum assuming a clear-sky atmosphere (panel A) and a cloudy atmosphere (panel B). Only the features corresponding to the most abundant species in the vertical gas profiles in Fig. 1 are shown in panels A and B. Each molecule’s set of features is expressed by a unique color while contributing to the grey area beneath the black line that corresponds to the total transmission spectrum. In the UV and visible, O_3 and N_2 (via Rayleigh scattering) are the main contributors to the spectrum. In the near and mid-infrared, many wide H_2O absorption bands are present, along with some weaker CH_4 bands. The CO_2 features have the strongest relative transit depth comparable to the O_3 feature at $9.6 \mu m$. Note that two collision-induced absorption (CIA) features are particularly notable on the spectrum: the N_2 - N_2 CIA at $4.3 \mu m$ (Schwieterman et al. 2015; Misra et al. 2014) and the O_2 - O_2 CIA at $6.4 \mu m$ (Fauchez et al. 2019c). The former overlaps the strong CO_2 feature and will be detectable only in the absence of CO_2 . Panel B is similar in model setup to panel A, except that panel B includes the spectral effects of clouds whose locations are predicted by the LMD-G GCM, placing them at 15 km. By comparing these effects to the clear-sky atmosphere, one can see a significant decrease in the relative transit depth of each line. It is noted that clouds are strongly opaque to the visible and infrared transmitted radiations. As a result, the spectral continuum is raised above the cloud deck where the atmosphere is semi-transparent (Fauchez et al. 2019a; Suissa et al. 2019a,b). Because the relative transit depth corresponds to the transit depth in the continuum subtracted from the transit depth in the line, a higher continuum reduces the relative transit depth.

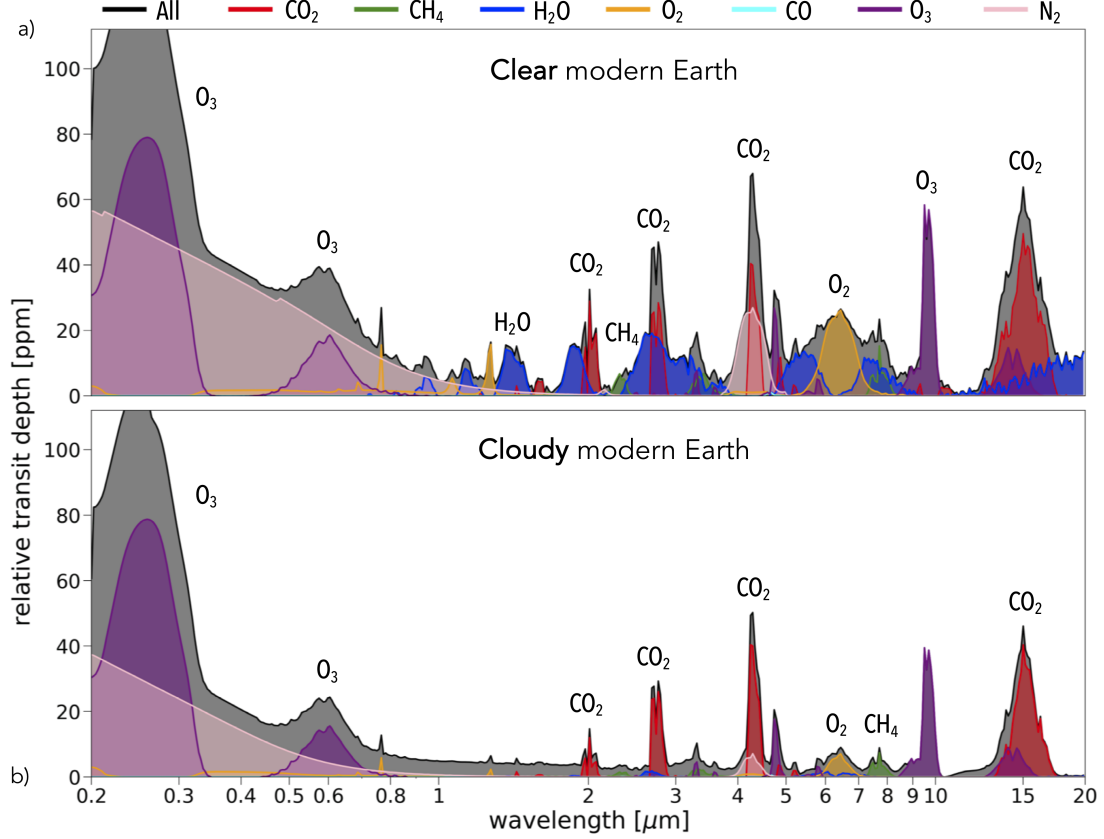


Figure 2. Simulated transmission spectrum of a modern Earth-like atmosphere on TRAPPIST-1e both in a clear-sky scenario (panel A) and in the presence of clouds placed by the LMD-G GCM (panel B). The sum of all gases is represented by a grey shade and the individual gaseous absorption of molecular features are represented by their corresponding colors.

H_2O is extremely affected by the presence of clouds because the H_2O vapor is mostly trapped beneath the cloud deck. This can also be seen in the H_2O profile in Fig. 1. Other gases are more well-mixed up to high altitudes far above the cloud deck and are therefore much less impacted by clouds than H_2O . Clouds are expected to be a recurrent feature of the atmospheres of terrestrial planets in the HZ, as liquid water on the surface would eventually evaporate and condense into the atmosphere. The opacity of clouds in the spectra poses a major obstacle in the atmospheric characterization of such planets (Komacek et al. 2019).

3.2. Detectability of a Modern Earth-like Atmosphere with Future Space-Based Observatories

Future space-based observatories such as *JWST* or concepts such as *HabEx*, *LUVOIR* and *Origins* would require the use of transmission spectroscopy to characterize the atmosphere of planets orbiting in the HZ of ultra-cool M dwarfs such as TRAPPIST-1. Direct imaging would not be possible for such close-in systems because of their inner working angle (IWA) and temperatures that are too cold to be characterizable via direct imaging (Lincowski et al. 2018; Lustig-Yaeger et al. 2019; Fauchez et al. 2019a). Fortunately, each of these future observatories would have at least one instrument with transmission spectroscopy capabilities. The characteristics of these instruments are summarized in Table 1.

Table 1. Wavelength range, instrument resolving power (R) and effective (Eff.) aperture size for *JWST* (NIRSpec Prism and MIRI), *LUVOIR*, *HabEx*, and *Origins*

Telescope	JWST		Origins	HabEx	LUVOIR-B	LUVOIR-A
Instrument	NIRSpec Prism	MIRI LRS	MISC-T	HWC	HDI	
Wavelength range (μm)	0.6 - 5.3	5.0 - 12.0	2.8 - 20	0.2 - 1.8	0.2 - 2.5	
R	100	100	50-100	1000	500 - 50,000	
Eff. aperture (m)	5.6		5.9	4.0	8.0	15.0

Figure 3 shows a simulated transmission spectrum for a cloudy-sky, modern Earth-like atmosphere on TRAPPIST-1e with the addition of the wavelength range covered by each instrument, as well as their noise expectations for 85 transits assuming a photon noise limited scenario. We see that depending on the telescopes and/or instruments, different spectral lines would be detectable. For instance, while LUVOIR has the largest aperture, its wavelength coverage (cf. Table 1) does not include the strongest CO₂ bands at 2.7 or 4.3 μm , and it operates in the spectral region where cloud opacity is the most prominent. As a result, the water and O₂ lines in this region are far too shallow to be detectable even with the largest aperture size.

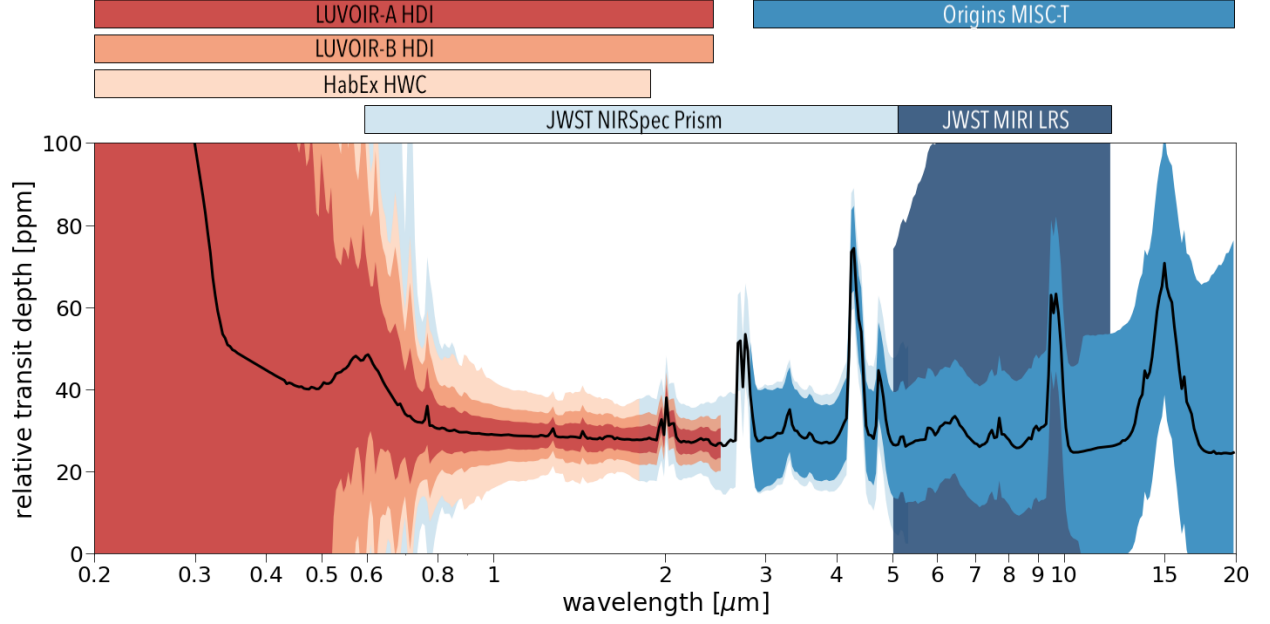


Figure 3. Simulated transmission spectrum for a cloudy-sky, modern Earth-like atmosphere on TRAPPIST-1e as would be observed with LUV0IR-A/B HDI, HabEx HWC, JWST NIRSpec Prism/MIRI LRS, and Origins MISC-T. The relative transit depth (black line), instrumental noise expectations (spectrum colors), and instrumental wavelength ranges (colored bars) are presented.

When instrument performances are compared, several parameters would be at play to detect specific molecular species:

- **Wavelength coverage:** Different spectral lines are accessible depending on the wavelength coverage of the instrument.
- **Resolving power (R):** $\lambda/\delta\lambda$ with λ the wavelength and $\delta\lambda$ the spectral resolution. Reducing R allows to increase the number of photons per spectral bands, reducing the noise. However, R should be high enough to spectrally resolve the width of the spectral feature. In this work we have optimized the resolving power by finding the lowest R to maximize the S/N.
- **Aperture size:** A larger aperture size collects more photons improving the S/N and therefore reducing the integration time needed to detect a given spectral feature.
- **Instrumental noise:** Noise produced by the instruments and the optics are wavelength dependent. Different technologies are used between *JWST*, *Origins*, *HabEx* and *LUV0IR-A/B*

that control the S/N. Such large telescopes will quickly acquire a significant number of photons after only a few transits and the noise from the source will largely dominate the total noise.

Figure 4 shows the signal-noise-ratios for each spectral feature after 85 transits of TRAPPIST-1e, corresponding to the expected visibility of the planet in a 5-year timespan. The clear sky atmosphere is shown for comparison but the analysis is performed on the cloudy atmosphere as it is the most realistic scenario for a habitable planet. In the presence of clouds, only CO₂ is detectable at a confidence level of 5 σ or more, for *JWST*'s NIRSpec Prism and *Origins*' MISC-T. This detection is possible due to the strong 4.3 μm CO₂ line (Lustig-Yaeger et al. 2019; Fauchez et al. 2019a).

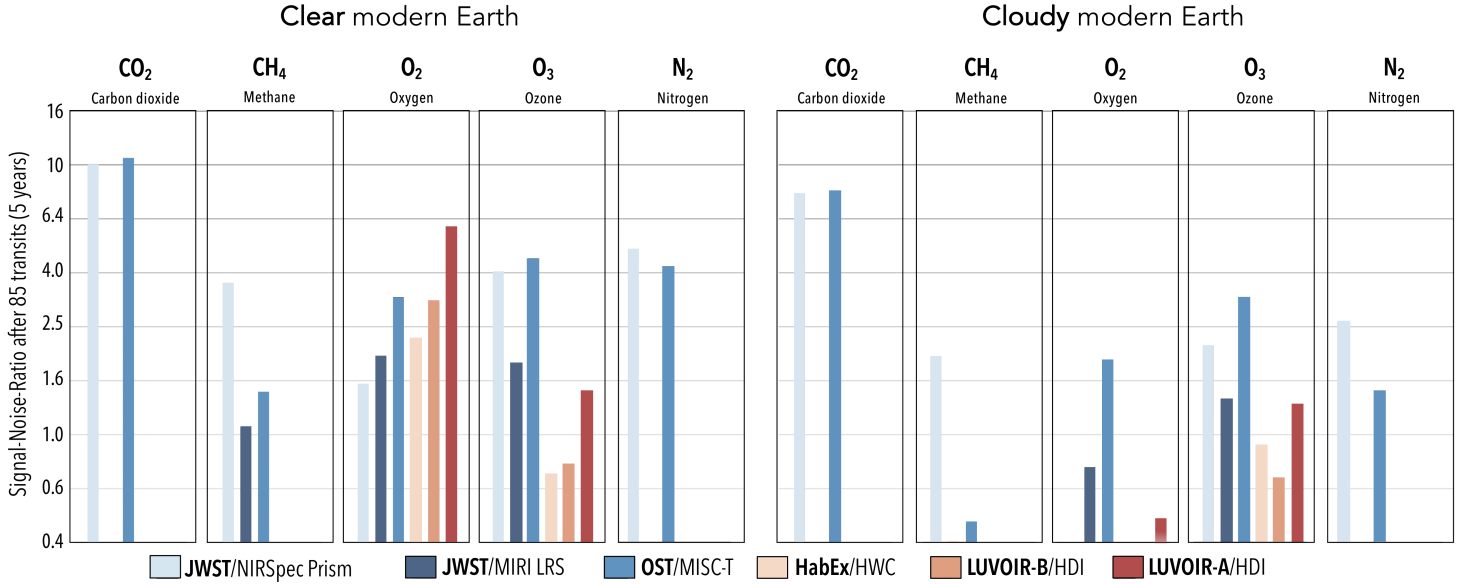


Figure 4. Comparison of Signal-Noise-Ratios (S/N) for the different molecular indicators and observatories assuming photon noise statistics. The values were computed assuming a 5-year time span, corresponding to a total of 85 observable transits of TRAPPIST-1e.

For the detection of O₃, the S/N of *LUVOIR-A* is twice as large as that of *LUVOIR-B* due to the increase of the aperture size from 8 to 15 m. Indeed, the S/N is proportional to the square root of the number n of collected photons (\sqrt{n}). Yet, the increase in the number n of photons collected

depends on the ratio between the radius squared of the two mirrors $(R_A/R_B)^2$ (assumed to be perfect disks), with R_A the radius of *LUVVOIR*-A (7.5 m) and R_B the radius of *LUVVOIR*-B (4 m). The S/N therefore improves by a factor $R_A/R_B=7.5/4=1.875$ between *LUVVOIR*-B and *LUVVOIR*-A.

Beyond collecting area and spectral coverage (photon noise statistics), the detector noise performance and systematic/calibration effects (e.g., "noise floors") will impact the detectability of a certain feature. For this investigation, our error analysis includes the detector properties as described by the observatory teams (e.g., read-noise [e-], dark current [e-/s], throughputs), while there is a large uncertainty on the actual limits or noise floors for these observatories. For *JWST*, [Deming et al. \(2009\)](#); [Greene et al. \(2016\)](#) have assumed 1σ noise floors for NIRSpec Prism and MIRI LRS of 20 and 50 ppm, respectively. However, the systematic behavior of detectors is continuously being improved, and we consider these values to be conservative. Future facilities such as *Origins*, *LUVVOIR*, and *HabEx* expect to achieve instrumental noise floors of 5 ppm or better ([Meixner et al. 2019](#); [TheLUVOIRTeam 2019](#); [Gaudi et al. 2018](#)). For this study, the TRAPPIST-1 system is bright enough to be dominated by photon noise statistics (not detector noise), and not bright enough (noise typically greater than 5-10 ppm) to be dominated by systematics (typically affecting low intrinsic noise and brighter sources), so detector properties and noise floors play a small role in establishing the detectability of the features presented here. Furthermore, there is a strong consensus that new calibration techniques and other analytical methods may lead to future reduction of these noise floors, and therefore we have not based our conclusions on these.

4. DISCUSSIONS

While planets orbiting M-dwarf stars have the benefit of very frequent transits, they endure several issues regarding their characterization. First, the planets are so close to their host star that they are unable to be observed in direct imaging as they would lie within the instrument's inner working angle. In addition, planets in the habitable zone are too temperate to be characterized during a secondary eclipse from their emission spectra. Therefore, only transmission spectroscopy can be used to characterize such planets. However, as shown in this work and in previous studies ([Morley](#)

et al. 2017; Fauchez et al. 2019a; Lustig-Yaeger et al. 2019; Suissa et al. 2019a,b; Komacek et al. 2019), atmospheric characterization through transmission spectroscopy would also be exceptionally challenging. At the mild temperatures of habitable planets, the atmospheric scale height is relatively small and the presence of clouds, inevitable if liquid water is present on the surface, strongly reduces the relative transit depth of all spectral features. These atmospheric transit depths could be on the order of or smaller than those due to stellar variability at certain wavelengths (spots, facula; Ducrot et al. (2018); Zhang et al. (2018); Rackham et al. (2018) and could therefore be difficult to disentangle. Also, the host star is so dim that the number of photons transmitted through the planet’s atmosphere is orders of magnitudes lower than for planets orbiting G-dwarfs. As a result, the S/N improves slowly with additional transits.

According to our simulations, if TRAPPIST-1e has an atmospheric composition similar to modern Earth, only CO₂ would be detectable at 4.3 μm . CO₂ is only detectable by either *JWST* or *Origins*, due to the fact that they are the only observatories with instruments capable of providing transit spectroscopy measurements that cover this wavelength range.

Synergies between instruments may be crucial in order to combine observations within various wavelength ranges and to accumulate transits over an extended period of time. For example, observations with future extremely large telescopes such as the *ELT*, *GMT*, or *TMT* using cross-correlation techniques are promising and should be used in conjunction with transit observations from space. Although it is unlikely that ground-based observations targeting H₂O, CO₂, or CH₄ in Earth-like planets could compete with those taken from space (e.g. Charbonneau & Deming 2007; Kaltenegger & Traub 2009), this is not the case for molecular O₂ (Snellen et al. 2013). Other sources of absorption in an Earth-like atmosphere are relatively isolated from the O₂ bands at 0.76 μm and 1.26 μm , allowing for the possibility of detection after a few dozen transits (Snellen et al. 2013). This could potentially allow for the detection of O₂ on a planet such as TRAPPIST-1e.

The importance of wavelength range and resolution is demonstrated by the strength of the detections of CH_4 . Of particular note is the stronger detections of CH_4 by *JWST*/NIRSpec, compared to *Origins*/MISC-T, despite the greater aperture of MISC-T. This is mainly due to the greater spectral resolution and spectral contrast achieved with *JWST*/NIRSpec. While none of these instruments or observatories can detect modern-day CH_4 for cloudy atmospheres, this may end up being important for planets with greater CH_4 concentrations, such as those thought to have been present on early Earth (Arney et al. 2016, 2017). This is especially important for any attempted search for biosignatures, as the combination of CH_4 and CO_2 might be the most detectable biosignature pairing for *JWST* (Krissansen-Totton et al. 2018).

5. CONCLUSIONS AND PERSPECTIVES

In this work, we have used TRAPPIST-1e, potentially the most promising target for atmospheric characterization of a planet in the HZ of a nearby M-dwarf, as a benchmark to compare expected transmission spectroscopy performances of future space-based observatories. This study does not aim to investigate the detectability of each gaseous species under various habitable conditions, such as those of Earth through time. Instead, we focus on the most well-known habitable atmospheric composition, that of modern Earth, and compare a variety of instrument capabilities to characterize individual molecular species. Our study shows that, despite the anticipation of tremendous future improvements in terms of aperture size and instrument performance, these factors would not be enough to characterize such planets via transmission spectroscopy. Indeed, most spectral lines from the gaseous species of a modern Earth-like atmosphere produce a relatively small transit depth and clouds drastically reduce their amplitude. Even for the largest aperture size of 15 m for *LUVOIR-A*, hundreds or thousands of observed transits would be required to detect molecular species at a 5σ confidence level via transit spectroscopy. Only CO_2 and its strongest feature at $4.3\text{ }\mu\text{m}$ could be detectable with a $\text{S/N} \geq 5$ in 85 transits, assuming all observable transits would be accrued during a 5 year mission. This feature would be observable with *JWST*'s NIRSpec Prism and with *Origins*' MISC-T. This spectral feature may be the only proxy available to detect the atmosphere of a rocky

HZ planet through transmission spectroscopy with currently-planned or conceptualized space-based telescopes.

This work therefore demonstrates that transmission spectroscopy may not be an appropriate technique to characterize habitable planets with a composition similar to modern Earth around M-dwarfs with a single telescope, or even with a combination of space-based assets. Instrumental and mission-level synergies between space- and ground-based telescopes should be prioritized in order to improve our chances to characterize such planets.

ACKNOWLEDGEMENTS

We thank our anonymous reviewer for their thoughtful analysis of our work, as their suggestions greatly improved the strength of our manuscript. This work was performed as a part of the NASA Astrobiology Institute’s Virtual Planetary Laboratory, supported by the National Aeronautics and Space Administration through the NASA Astrobiology Institute under solicitation No. 80NSSC18K0829. All authors acknowledge support from the NASA Goddard Space Flight Center (GSFC) Sellers Exoplanet Environments Collaboration (SEEC), which is funded in part by the NASA Planetary Science Division’s Internal Scientist Funding Model.

Software: Atmos ([Arney et al. 2016](#)), LMD-G ([Wordsworth et al. 2011](#)), PSG ([Villanueva et al. 2018](#))

REFERENCES

- | | |
|---|--|
| <p>Anglada-Escudé, G., Amado, P. J., Barnes, J.,
et al. 2016, <i>Nature</i>, 536, 437,
doi: 10.1038/nature19106</p> <p>Arney, G., Domagal-Goldman, S. D., Meadows,
V. S., et al. 2016, <i>Astrobiology</i>, 16, 873,
doi: 10.1089/ast.2015.1422</p> | <p>Arney, G. N., Meadows, V. S., Domagal-Goldman,
S. D., et al. 2017, <i>ApJ</i>, 836, 49,
doi: 10.3847/1538-4357/836/1/49</p> |
|---|--|

- Bagnasco, G., Kolm, M., Ferruit, P., et al. 2007, in Society of Photo-Optical Instrumentation Engineers (SPIE) Conference Series, Vol. 6692, Proc. SPIE, 66920M
- Barstow, J. K., & Irwin, P. G. J. 2016, Monthly Notices of the Royal Astronomical Society, 461, L92, doi: [10.1093/mnrasl/slw109](https://doi.org/10.1093/mnrasl/slw109)
- Battersby, C., Armus, L., Bergin, E., et al. 2018, Nature Astronomy, 2, 596, doi: [10.1038/s41550-018-0540-y](https://doi.org/10.1038/s41550-018-0540-y)
- Benneke, B., Wong, I., Piaulet, C., et al. 2019a, ApJL, 887, L14, doi: [10.3847/2041-8213/ab59dc](https://doi.org/10.3847/2041-8213/ab59dc)
- Benneke, B., Knutson, H. A., Lothringer, J., et al. 2019b, Nature Astronomy, 3, 813, doi: [10.1038/s41550-019-0800-5](https://doi.org/10.1038/s41550-019-0800-5)
- Bouchet, P., García-Marín, M., Lagage, P. O., et al. 2015, PASP, 127, 612, doi: [10.1086/682254](https://doi.org/10.1086/682254)
- Bourrier, V., Lecavelier des Etangs, A., Ehrenreich, D., et al. 2018, Astronomy & Astrophysics, 620, A147, doi: [10.1051/0004-6361/201833675](https://doi.org/10.1051/0004-6361/201833675)
- Burdanov, A., Delrez, L., Gillon, M., & Jehin, E. 2018, Handbook of Exoplanets, 10071023, doi: [10.1007/978-3-319-55333-7_130](https://doi.org/10.1007/978-3-319-55333-7_130)
- Burdanov, A. Y., Lederer, S. M., Gillon, M., et al. 2019, MNRAS, 487, 1634, doi: [10.1093/mnras/stz1375](https://doi.org/10.1093/mnras/stz1375)
- Charbonneau, D., & Deming, D. 2007, The Dynamics-Based Approach to Studying Terrestrial Exoplanets. <https://arxiv.org/abs/0706.1047>
- de Wit, J., Wakeford, H. R., Gillon, M., et al. 2016, Nature, 537, 69 EP
- de Wit, J., Wakeford, H. R., Lewis, N. K., et al. 2018, Nature Astronomy, 2, 214, doi: [10.1038/s41550-017-0374-z](https://doi.org/10.1038/s41550-017-0374-z)
- Delrez, L., Gillon, M., Triaud, A. H. M. J., et al. 2018, Monthly Notices of the Royal Astronomical Society, 475, 3577, doi: [10.1093/mnras/sty051](https://doi.org/10.1093/mnras/sty051)
- Deming, D., Seager, S., Winn, J., et al. 2009, Publications of the Astronomical Society of the Pacific, 121, 952, doi: [10.1086/605913](https://doi.org/10.1086/605913)
- Diamond-Lowe, H., Berta-Thompson, Z., Charbonneau, D., Dittmann, J., & Kempton, E. M.-R. 2020, The Astronomical Journal, 160, 27, doi: [10.3847/1538-3881/ab935f](https://doi.org/10.3847/1538-3881/ab935f)
- Diamond-Lowe, H., Berta-Thompson, Z., Charbonneau, D., & Kempton, E. M. R. 2018, AJ, 156, 42, doi: [10.3847/1538-3881/aac6dd](https://doi.org/10.3847/1538-3881/aac6dd)
- Dressing, C. D., & Charbonneau, D. 2015, The Astrophysical Journal, 807, 45, doi: [10.1088/0004-637x/807/1/45](https://doi.org/10.1088/0004-637x/807/1/45)
- Ducrot, E., Sestovic, M., Morris, B. M., et al. 2018, The Astronomical Journal, 156, 218, doi: [10.3847/1538-3881/aade94](https://doi.org/10.3847/1538-3881/aade94)
- Ducrot, E., Gillon, M., Delrez, L., et al. 2020, arXiv e-prints, arXiv:2006.13826. <https://arxiv.org/abs/2006.13826>
- Evans, T. M., Sing, D. K., Goyal, J. M., et al. 2018, AJ, 156, 283, doi: [10.3847/1538-3881/aaebff](https://doi.org/10.3847/1538-3881/aaebff)

- Fauchez, T., Turbet, M., Wolf, E. T., et al. 2019b, Geoscientific Model Development Discussions, 2019, 1, doi: [10.5194/gmd-2019-166](https://doi.org/10.5194/gmd-2019-166)
- Fauchez, T., Villanueva, G., Schwieterman, E., et al. 2019c, Nature Astronomy, accepted, doi: [10.1038/s41550-019-0977-7](https://doi.org/10.1038/s41550-019-0977-7)
- Fauchez, T. J., Turbet, M., Villanueva, G. L., et al. 2019a, Accepted to The Astrophysical Journal
- Ferruit, P., Birkmann, S., Böker, T., et al. 2014, in Society of Photo-Optical Instrumentation Engineers (SPIE) Conference Series, Vol. 9143, Proc. SPIE, 91430A
- Gaudi, B. S., Seager, S., Mennesson, B., et al. 2018, arXiv e-prints, arXiv:1809.09674. <https://arxiv.org/abs/1809.09674>
- Gibson, N. P., Aigrain, S., Barstow, J. K., et al. 2013, MNRAS, 436, 2974, doi: [10.1093/mnras/stt1783](https://doi.org/10.1093/mnras/stt1783)
- Gillon, M. 2018, Nature Astronomy, 2, 344, doi: [10.1038/s41550-018-0443-y](https://doi.org/10.1038/s41550-018-0443-y)
- Gillon, M., Jehin, E., Lederer, S. M., et al. 2016, Nature, 533, 221
- Gillon, M., Triaud, A. H. M. J., Demory, B.-O., et al. 2017, Nature, 542, 456460
- Gordon, I., Rothman, L., Hill, C., et al. 2017, J QUANT SPECTROSC RA, 203, 3 , doi: <https://doi.org/10.1016/j.jqsrt.2017.06.038>
- Greene, T. P., Line, M. R., Montero, C., et al. 2016, The Astrophysical Journal, 817, 17, doi: [10.3847/0004-637X/817/1/17](https://doi.org/10.3847/0004-637X/817/1/17)
- Grimm, S. L., Demory, B.-O., Gillon, M., et al. 2018, Astronomy and Astrophysics, 613, A68, doi: [10.1051/0004-6361/201732233](https://doi.org/10.1051/0004-6361/201732233)
- Kaltenegger, L., Miguel, Y., & Rugheimer, S. 2012, International Journal of Astrobiology, 11, 297307, doi: [10.1017/S1473550412000134](https://doi.org/10.1017/S1473550412000134)
- Kaltenegger, L., & Traub, W. A. 2009, The Astrophysical Journal, 698, 519, doi: [10.1088/0004-637X/698/1/519](https://doi.org/10.1088/0004-637X/698/1/519)
- Kasting, J. F., Whitmire, D. P., & Reynolds, R. T. 1993, Icarus, 101, 108 , doi: <https://doi.org/10.1006/icar.1993.1010>
- Keller-Rudek, H., Moortgat, G. K., Sander, R., & Sörensen, R. 2013, Earth System Science Data, 5, 365, doi: [10.5194/essd-5-365-2013](https://doi.org/10.5194/essd-5-365-2013)
- Kendrew, S., Scheithauer, S., Bouchet, P., et al. 2015, PASP, 127, 623, doi: [10.1086/682255](https://doi.org/10.1086/682255)
- Knutson, H. A., Benneke, B., Deming, D., & Homeier, D. 2014, Nature, 505, 66, doi: [10.1038/nature12887](https://doi.org/10.1038/nature12887)
- Komacek, T. D., Fauchez, T. J., Wolf, E. T., & Abbot, D. S. 2019, Accepted in ApJ letters, doi: [10.1007/s11214-018-0575-5](https://doi.org/10.1007/s11214-018-0575-5)
- Kopparapu, R. K., Ramirez, R., Kasting, J. F., et al. 2013, The Astrophysical Journal, 765, 131
- Kreidberg, L., Bean, J. L., Désert, J.-M., et al. 2014, Nature, 505, 69, doi: [10.1038/nature12888](https://doi.org/10.1038/nature12888)
- Krissansen-Totton, J., Bergsman, D. S., & Catling, D. C. 2016, Astrobiology, 16, 39
- Krissansen-Totton, J., Garland, R., Irwin, P., & Catling, D. C. 2018, AJ, 156, 114, doi: [10.3847/1538-3881/aad564](https://doi.org/10.3847/1538-3881/aad564)

- Liebert, J., & Gizis, J. E. 2006, Publications of the Astronomical Society of the Pacific, 118, 659, doi: [10.1086/503333](https://doi.org/10.1086/503333)
- Lincowski, A. P., Meadows, V. S., Crisp, D., et al. 2018, The Astrophysical Journal, 867, 76, doi: [10.3847/1538-4357/aae36a](https://doi.org/10.3847/1538-4357/aae36a)
- Lindgren, L., Hernández, J., Bombrun, A., et al. 2018, A&A, 616, A2, doi: [10.1051/0004-6361/201832727](https://doi.org/10.1051/0004-6361/201832727)
- Luger, R., Sestovic, M., Kruse, E., et al. 2017, Nature Astronomy, 1, 0129, doi: [10.1038/s41550-017-0129](https://doi.org/10.1038/s41550-017-0129)
- Lustig-Yaeger, J., Meadows, V. S., & Lincowski, A. P. 2019, The Astronomical Journal, 158, 27, doi: [10.3847/1538-3881/ab21e0](https://doi.org/10.3847/1538-3881/ab21e0)
- Meadows, V. S., Arney, G. N., Schwieterman, E. W., et al. 2018, Astrobiology, 18, 133, doi: [10.1089/ast.2016.1589](https://doi.org/10.1089/ast.2016.1589)
- Meixner, M., Cooray, A., Leisawitz, D., et al. 2019. <https://arxiv.org/abs/1912.06213>
- Misra, A., Meadows, V., Claire, M., & Crisp, D. 2014, Astrobiology, 14, 67
- Moran, S. E., Hrst, S. M., Batalha, N. E., Lewis, N. K., & Wakeford, H. R. 2018, The Astronomical Journal, 156, 252
- Morley, C. V., Kreidberg, L., Rustamkulov, Z., Robinson, T., & Fortney, J. J. 2017, The Astrophysical Journal, 850, 121, doi: [10.3847/1538-4357/aa927b](https://doi.org/10.3847/1538-4357/aa927b)
- Morris, B. M., Agol, E., Hebb, L., et al. 2018, ApJL, 863, L32, doi: [10.3847/2041-8213/aad8aa](https://doi.org/10.3847/2041-8213/aad8aa)
- Nikolov, N., Sing, D. K., Burrows, A. S., et al. 2015, Monthly Notices of the Royal Astronomical Society, 447, 463, doi: [10.1093/mnras/stu2433](https://doi.org/10.1093/mnras/stu2433)
- Pallé, E. 2018, The Detectability of Earth's Biosignatures Across Time (Springer International Publishing AG, part of Springer Nature), 70, doi: [10.1007/978-3-319-55333-7_70](https://doi.org/10.1007/978-3-319-55333-7_70)
- Pont, F., Sing, D. K., Gibson, N. P., et al. 2013, MNRAS, 432, 2917, doi: [10.1093/mnras/stt651](https://doi.org/10.1093/mnras/stt651)
- Rackham, B. V., Apai, D., & Giampapa, M. S. 2018, ApJ, 853, 122, doi: [10.3847/1538-4357/aaa08c](https://doi.org/10.3847/1538-4357/aaa08c)
- Rajpurohit, A. S., Reylé, C., Allard, F., et al. 2013, Astronomy & Astrophysics, 556, A15, doi: [10.1051/0004-6361/201321346](https://doi.org/10.1051/0004-6361/201321346)
- Schwieterman, E. W., Robinson, T. D., Meadows, V. S., Misra, A., & Domagal-Goldman, S. 2015, The Astrophysical Journal, 810, 57, doi: [10.1088/0004-637x/810/1/57](https://doi.org/10.1088/0004-637x/810/1/57)
- Seager, S., & Deming, D. 2010, Annual Review of Astronomy and Astrophysics, 48, 631672, doi: [10.1146/annurev-astro-081309-130837](https://doi.org/10.1146/annurev-astro-081309-130837)
- Sing, D. K., Pont, F., Aigrain, S., et al. 2011, MNRAS, 416, 1443, doi: [10.1111/j.1365-2966.2011.19142.x](https://doi.org/10.1111/j.1365-2966.2011.19142.x)
- Sing, D. K., Lecavelier des Etangs, A., Fortney, J. J., et al. 2013, MNRAS, 436, 2956, doi: [10.1093/mnras/stt1782](https://doi.org/10.1093/mnras/stt1782)
- Sing, D. K., Wakeford, H. R., Showman, A. P., et al. 2015, MNRAS, 446, 2428, doi: [10.1093/mnras/stu2279](https://doi.org/10.1093/mnras/stu2279)

- Sing, D. K., Fortney, J. J., Nikolov, N., et al. 2016, *Nature*, 529, 59, doi: [10.1038/nature16068](https://doi.org/10.1038/nature16068)
- Snellen, I. A. G., de Kok, R. J., le Poole, R., Brogi, M., & Birkby, J. 2013, *The Astrophysical Journal*, 764, 182, doi: [10.1088/0004-637X/764/2/182](https://doi.org/10.1088/0004-637X/764/2/182)
- Southworth, J., Mancini, L., Madhusudhan, N., et al. 2017, *The Astronomical Journal*, 153, 191, doi: [10.3847/1538-3881/aa6477](https://doi.org/10.3847/1538-3881/aa6477)
- Steele, I. A., Smith, R. J., Rees, P. C., et al. 2004, in *Society of Photo-Optical Instrumentation Engineers (SPIE) Conference Series*, Vol. 5489, Proc. SPIE, ed. J. Oschmann, Jacobus M., 679–692
- Suissa, G., Mandell, A., Wolf, E., et al. 2019a, Accepted in the *Astrophysical Journal*
- Suissa, G., Wolf, E. T., Kopparapu, R. K., et al. 2019b, Accepted in the *Astrophysical Journal*
- TheLUVOIRTeam. 2019. <https://arxiv.org/abs/1912.06219>
- Turbet, M., Forget, F., Head, J. W., & Wordsworth, R. 2017, *Icarus*, 288, 10, doi: [10.1016/j.icarus.2017.01.024](https://doi.org/10.1016/j.icarus.2017.01.024)
- Turbet, M., Bolmont, E., Leconte, J., et al. 2018, *Astronomy and Astrophysics*, 612, A86, doi: [10.1051/0004-6361/201731620](https://doi.org/10.1051/0004-6361/201731620)
- Vanderburg, A., Rowden, P., Bryson, S., et al. 2020, *The Astrophysical Journal*, 893, L27, doi: [10.3847/2041-8213/ab84e5](https://doi.org/10.3847/2041-8213/ab84e5)
- Villanueva, G. L., Smith, M. D., Protopapa, S., Faggi, S., & Mandell, A. M. 2018, *Journal of Quantitative Spectroscopy and Radiative Transfer*, 217, 86, doi: [10.1016/j.jqsrt.2018.05.023](https://doi.org/10.1016/j.jqsrt.2018.05.023)
- Wakeford, H. R., Sing, D. K., Deming, D., et al. 2018, *AJ*, 155, 29, doi: [10.3847/1538-3881/aa9e4e](https://doi.org/10.3847/1538-3881/aa9e4e)
- Wolf, E. T. 2017, *The Astrophysical Journal Letters*, 839, L1
- Wordsworth, R. D., Forget, F., Selsis, F., et al. 2011, *The Astrophysical Journal Letters*, 733, L48
- Zhang, Z., Zhou, Y., Rackham, B. V., & Apai, D. 2018, *The Astronomical Journal*, 156, 178, doi: [10.3847/1538-3881/aade4f](https://doi.org/10.3847/1538-3881/aade4f)